

Loughborough University
Institutional Repository

*Effects of particle surface
properties on filter cake
formation and consolidation*

This item was submitted to Loughborough University's Institutional Repository by the/an author.

Citation: WAKEMAN, R.J., TARLETON, E.S. and SABRI, M.N., 1993. Effects of particle surface properties on filter cake formation and consolidation. IN: Proceedings of the 6th World Filtration Congress, Nagoya, Japan, May 1993, pp.930-935

Additional Information:

- This is a conference paper.

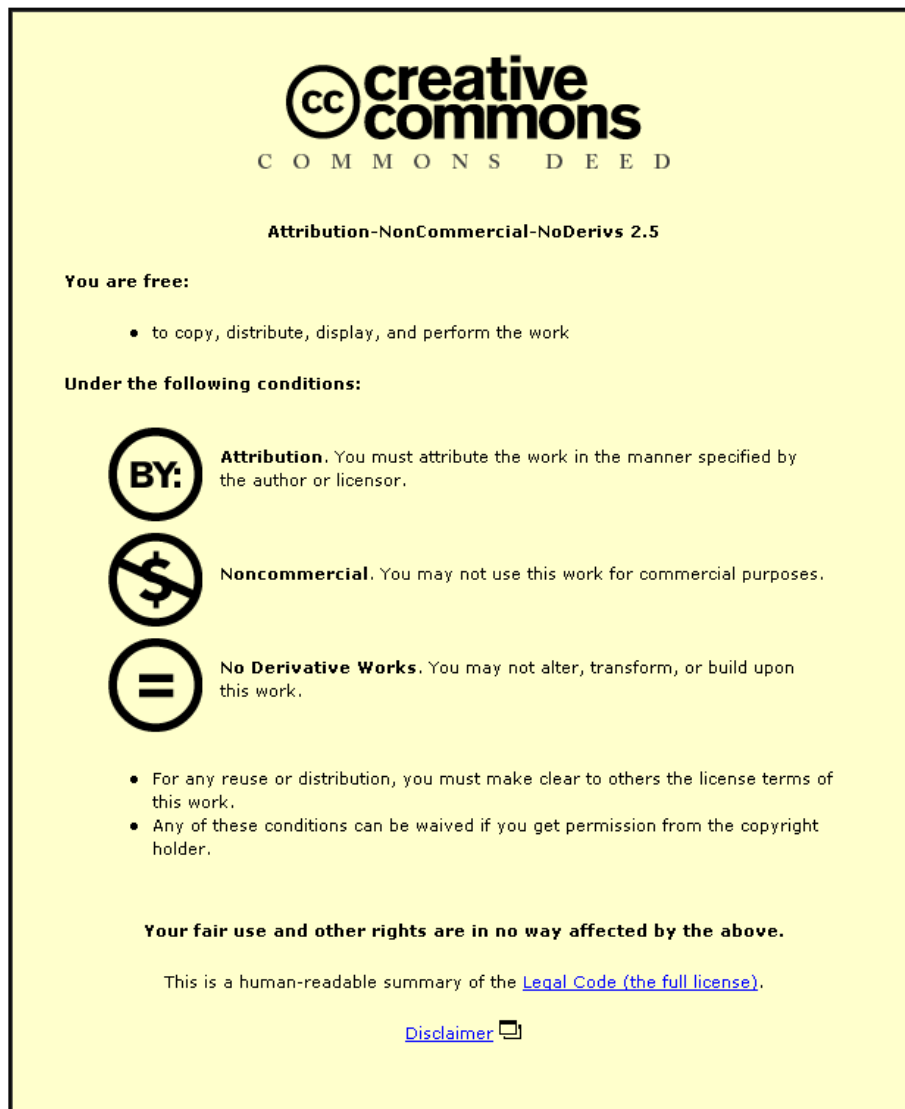
Metadata Record: <https://dspace.lboro.ac.uk/2134/5605>

Version: Accepted for publication

Publisher: Nagoya Industrial Science Research Institute (NISRI)

Please cite the published version.

This item was submitted to Loughborough's Institutional Repository (<https://dspace.lboro.ac.uk/>) by the author and is made available under the following Creative Commons Licence conditions.



For the full text of this licence, please go to:
<http://creativecommons.org/licenses/by-nc-nd/2.5/>

EFFECTS OF PARTICLE SURFACE PROPERTIES ON FILTER CAKE FORMATION AND CONSOLIDATION

R.J. Wakeman¹, E.S. Tarleton² (e.s.tarleton@lboro.ac.uk) and M.N. Sabri¹

¹School of Engineering, Exeter University, Exeter EX4 4QF, UK.

²Dept. of Chemical Engineering, Loughborough University, Loughborough, LE11 3TU, UK.

ABSTRACT

Data are reported on the formation of filter cakes under pressure where the particles are largely finer than about 10 μm . The data are analysed through two consecutive mechanisms, filtration and consolidation. Process design parameters for each mechanism are obtained, which will allow calculations to be made from small scale experiments. The magnitude and dependence of the constitutive parameters on pressure, pH, particle size and shape, and the nature of the particle-particle interactions are shown.

INTRODUCTION

In the process engineering related literature there is a lot of data which report the compression characteristics of solid/liquid mixtures; much of this has been collated by Shirato *et al.*¹. The main drawback with these earlier experiments is that none report all the relevant data pertaining to the particles and their solution environment, and it is therefore not possible to know which properties of the mixture affect compression. There is similarly a considerable amount of data in the colloid science literature (see, for example, in Hunter^{2,3} or Otterwill⁴) which has generally been obtained using 'ideal' particles (such as latices), and naturally greater emphasis has been placed upon the packing state of the particles and the formulation of inter-particle forces. These works have given considerable insight into the fundamental parameters, but have not yielded engineering or design data of practical significance. The experimental work here was therefore aimed at providing an understanding of the effects of fundamental properties on design data obtained for particulates which have some industrial significance. Some details of the experimental procedures and the wider implications of basic particle properties on laboratory studies and solid/liquid separation processes have been reported previously^{5,6,7}.

RELEVANT THEORY

The theory used to analyse the experimental data to give design information was largely developed by Shirato *et al.*⁸, together with the inclusion of some refinements and additions⁷. The compression of a stable suspension is made up of two parts, an initial stage in which filtration to form a cake occurs, followed by a consolidation stage during which the bulk volume of the deposited cake is reduced. The equation describing the filtration period is the conventional filtration equation:

$$\frac{1}{A} \frac{dV}{dt} = \frac{A\Delta p}{\mu(acV + AR)} \quad (1)$$

However, the integrated form of this equation is generally more convenient to use as the expelled liquid data are usually collected as volumes rather than flow rates. The integrated form of equation (1) at constant pressure is

$$\frac{t - t_i}{V - V_i} = \frac{K_1}{2}(V + V_i) + K_2 \quad (2)$$

where $K_1 = \alpha\mu/A^2\Delta p$ and $K_2 = \mu R/A\Delta p$. Plotting the data from the filtration stage as $(t - t_i)/(V - V_i)$ against $(V + V_i)$ leads to a straight line from which the cake properties characterising the rate of the first stage of formation may be evaluated; when the start of filtration coincides with the start of the integration, $t_i = V_i = 0$. The effective concentration of solids in the feed to be used in equations (1) and (2) is given by:

$$c = \frac{\rho s}{1 - ms} \quad (3)$$

where m is evaluated at the transition from slurry filtration to cake consolidation, i.e. at $m = m_1$.

The consolidation period, $L < L_1$, is analysed through the use of an empirical relationship relating the consolidation ratio

$$U_c = \frac{L_1 - L}{L_1 - L_\infty} \quad (4)$$

to a dimensionless consolidation time defined by

$$T_c = \frac{i^2 C_e t_c}{\omega_0^2} \quad (5)$$

where i is the number of drainage surfaces, C_e is a 'modified' consolidation coefficient, and t_c is the consolidation time ($t_c = 0$ at $U_c = 0$, i.e. at $L = L_1$). Sivaram and Swamee⁹ developed a parametric expression which approximated the solution to the Terzaghi^{10,11} model to within 3%, and that relationship was slightly modified by Shirato *et al.*⁸ to:

$$U_c = \frac{\sqrt{4T_c/\pi}}{\left(1 + (4T_c/\pi)^\nu\right)^{0.5\nu}} \quad (6)$$

where ν is the consolidation behaviour index which takes secondary consolidation effects into account. The Sivaram and Swamee⁹ equation takes no account of the effects of creep, and the behaviour index was assigned a constant value of 2.85. The rationale for $\nu = 2.85$ was simply that it fitted the Terzaghi model equations, but experimental data suggest that $\nu > 2.85$ is a reality⁷.

A value for C_e is obtained from the initial slope of the plot of U_c vs. t_c . For $T_c \ll 1$

$$U_c = \sqrt{\frac{4}{\pi} T_c} \quad (7)$$

and

$$K_e = (\text{slope})^2 = \frac{4i^2 C_e}{\pi \omega_0^2} \quad (8)$$

from which C_e is calculated.

RESULTS AND DISCUSSION

Pressure was found to have a large effect on some suspensions, but a fairly minor one on others. In general terms higher pressures lead to the more rapid formation of more densely packed cakes, but such statements must be qualified by the magnitude of the surface charge on the particles. Two examples of the effects of pressure are shown in Figures 1 and 2. Figure 2 shows pressure affecting the rate of expression to a much greater extent than it does the final packing density, whereas Figure 1 shows the converse with the final solids volume fraction being affected to a much greater extent than the rate. The reasons for these different behaviours lie with the range over which the inter-particle forces extend. Hydromagnesite is a composite of MgCO_3 , $\text{Mg}(\text{OH})_2$ and water of hydration and the magnitude of the pressures existing between the particles at high separation distances (~ 300 nm at 0.4 volume fraction) presents a problem which might only be explained by (a) a double layer charge being given by the lattice charge of the mineral, or (b) a thick layer of structured water over the particle surface. The diffuse double layer then originates at this distance from the surface. The lattice charge would need to correspond to a much higher surface potential than zeta potential measurements would suggest. It is difficult to reconcile the magnitude of the inter-particle pressures observed with expectations from double layer theory when considering the hydromagnesite data.

Effects of pH on expression were found to vary according to the magnitude of the surface charge on the particles. Calcite had a low zeta potential ($< |20|$ mV) and the repulsive forces are correspondingly low. As might be expected, calcite data showed negligible effects of pH on either the rate of expression or the final porosity of the cake. At the other extreme, the magnitude of the zeta potential of anatase (up to $\sim |60|$ mV) caused marked changes in the rate of expression, as shown on Figure 3. Most rapid expression occurred at the point of zero charge, whereas at greater (either positive or negative) zeta potentials the rate of compaction was reduced. At the lower pH on Figure 3 the ionic strength is high, thereby causing suppression of the double layer and a reduction in the magnitude of the repulsive force. The effects of pH (through the double layer thickness) on the final packing density appeared to be small in comparison with the effects demonstrated by the surface of hydromagnesite.

Experimental data from the piston press were available in the form of the volume of liquid expelled (V) or the piston displacement as a function of time (t). From these data and the conditions of the experiment it was necessary to evaluate the specific cake resistance (α) during the filtration stage of the expression process, and the modified consolidation coefficient (C_e) and the behaviour index (C_e) during the consolidation stage. These are the factors to be used in any subsequent design calculations. The voids ratio (e) in equilibrium with the applied pressure gives a measure of the limiting packing density achievable at that pressure. From analyses of several compression tests carried out at different pressures in the piston press, the parameters and voids ratio can be plotted as functions of the applied pressure Δp . Useful expressions for these purposes are only valid over a specified pressure range and take the form

$$\alpha = \alpha_0 \Delta p^n \quad (9)$$

$$e = e_0 - b \log(p) \quad (10)$$

where α_0 , n , e_0 and b are coefficients of the solid/liquid system of interest, α is the specific resistance of the deposit formed during the filtration stage and e is the voids ratio of the compact at the end of the compression process. Typical examples of the α vs. p relationships are shown on Figures 4 and 5, illustrating the decrease in permeability associated with smaller particle sizes and higher applied pressures. The permeability similarly decreases when the particles are better dispersed; changing the pH of the china clay suspension from 2.9 ($\zeta \sim 15$ mV) to 10.2 ($\zeta \sim 57$ mV) increases the specific resistance by a factor of about one order of magnitude.

Examples of the e vs. p relationships are shown on Figures 6 and 7. pH or surface charge appears to have no effect on the equilibrium voids ratio at these higher pressures, but reducing the

particle size (at a constant pH) results in a higher equilibrium voids ratio. This is presumably a manifestation of the greater charge density around the surface of the finer particles.

The coefficients characterising the compression phase of the operation, C_e and ν , are also known from the piston press results and may be represented by the equations:

$$C_e = C_{e0} p^\nu \quad (11)$$

$$\nu = \frac{4p}{\delta + p} \quad (12)$$

Coefficients arising from applications of the constitutive equations to the experimental data are summarised in Table 1. The limiting value of ν at high pressures is 4 according to equation (12), but it is recognised that ν is likely to be pressure dependent at lower applied pressures or when resisting forces between the particles are unusually high.

The data in Table 1 generally show the trends which might be anticipated, but there are also some unexpected results. The specific resistance increases and the cake voids ratio decreases with increasing pressure. Over the limited pressure range of the calcite tests there was not a detectable change in the compact permeability or specific resistance, in spite of a reduction of the voids ratio.

The less obvious results arise from expression of the anatase and hydromagnesite beds. For china clay the modified consolidation coefficient (C_e) increases with pressure, with a much increased sensitivity to pressure being observed at greater $|\zeta|$ potentials, but the consolidation behaviour index (ν) was constant. However, for anatase both the modified consolidation coefficient and the consolidation behaviour index were found to be independent of pressure; a value of the packing density close to the limit measured at the end of the experiment was obtained whilst the filtration mechanism was effective, leaving little potential for further consolidation of the compact. The most curious was the reduction of C_e with increasing pressure for hydromagnesite, together with the dependence of ν on pressure.

The different behaviour of hydromagnesite requires further consideration, as it may be attributed to various causes. The shape of the hydromagnesite particle is similar to that of a calcite particle and not too dissimilar from that of an anatase particle, and the surface charge is similar to that at a calcite surface. However, the size of the hydromagnesite particle is much greater than that of calcite or anatase and significant surface charge effects would not be expected to arise. A notable difference between the three particle systems is their solubility in cold water: anatase is insoluble, calcite has a solubility of 0.0014 g/100 ml, and hydromagnesite 0.04 g/100 ml. The solubility for hydromagnesite is greater than the corresponding solubility of either the carbonate (0.0106 g/100 ml) or hydroxide (0.0009 g/100 ml) in isolation, and could be expected to increase the electrolyte concentration near to the particle surfaces. If this led to a layer of structured liquid over the surface of the particle, it may explain why such anomalous results were obtained.

It is worth pointing out the effects of increasing the surface charge on the compaction process. Comparisons between the calcite and china clay data are particularly suitable for this: for calcite $\zeta \sim 16$ mV at pH = 11.8, and for china clay $\zeta \sim 57$ mV at pH = 2.9 and $\zeta \sim 15$ mV at pH = 2.9. The effect of charge alone is seen by comparing the china clay data at pH's 10.2 and 2.9. The ultimate packing densities at the two pH's are not very different, as shown by the e and b values on Table 1 and by Figure 6, but a higher surface charge considerably increases the resistance to cake formation, shown by the α_0 values. The effect of higher surface charges slowing the kinetics of formation is also demonstrated clearly for an unwashed anatase on Figure 3.

CONCLUDING REMARKS

The nature of the expression of fine particle suspensions is dependent on pH, particle size and shape, and the nature of the particle-particle interactions. The form of dynamic compaction curves can vary widely, but they can all be analysed through the application of a two stage mechanism model. The two stages, which act consecutively, are the basic filtration and consolidation processes. New data have been presented for some selected solid/liquid systems to show how the expression characteristics change with the basic and fundamental properties of the solid/liquid mixture.

ACKNOWLEDGEMENTS

The authors wish to acknowledge receipts of grants from the International Fine Particle Research institute in support of this work.

REFERENCES

1. M. Shirato, T. Murase, F.M. Tiller and A.F. Alciatore, 1981, in *Filtration*, M.J. Matteson and C. Orr (Eds.), Marcel Dekker, New York.
2. R.J. Hunter, 1981, *The Zeta Potential in Colloid Science*, Academic Press, London.
3. R.J. Hunter, 1987, *Foundations of Colloid Science*, Clarendon Press, Oxford.
4. R.H. Ottewill, 1980, Direct measurements of particle-particle interactions, *Progr. Colloid & Polymer Science*, **57**, 71.
5. S.T. Thuraisingham and R.J. Wakeman, 1987, *Proc. 20th Biennial Conf. of the International Briquetting Association*, pp.389-401.
6. R.J. Wakeman, S.T. Thuraisingham and E.S. Tarleton, 1989, *Filtration and Separation*, **26(4)**, 277.
7. R.J. Wakeman, M.N. Sabri and E.S. Tarleton, 1991, Factors affecting the formation and properties of wet compacts, *Powder Technology*, **65**, 283.
8. M. Shirato, T. Murase and M. Iwata, 1986, in *Progress in Filtration and Separation 4*, R.J. Wakeman (Ed.), Elsevier, Amsterdam.
9. B. Sivaram and P.K. Swamee, 1977, *J. Japanese Soc. Soil Mech. Found. Eng.*, **17**, 48.
10. K. Terzaghi and P.B. Peck, 1948, *Soil Mechanics in Engineering Practice*, Wiley, New York.
11. D.W. Taylor, 1962, *Fundamentals of Soil Mechanics*, 5th Edn., pp.225-229, Wiley, New York.

FIGURES AND TABLES

Particle type	pH	ϵ_{s0}	$X_{av}^{(1)}$	$\alpha_0^{(2)}$	n	e_0	b	$C_{e0}^{(3)}$	γ	$\delta^{(4)}$	
Anatase*	4.0	0.035	0.5	7.161×10^{11}	0.222	1.681	0.134	3.533×10^{-11}	0.915	0	
	7.0	0.01	0.5	5.353×10^{12}	0.027	5.916	0.318	1.657×10^{-12}	1.093	0	
	9.1	0.01	0.5	3.498×10^{12}	0.111	8.787	1.222	9.352×10^{-12}	0.912	0	
Aragonite**	11.0	0.04	1.7	1.382×10^{11}	0.227	4.286	0.687	1.869×10^{-10}	1.098	0	
	11.0	0.04	3.3	4.795×10^{10}	0.214	4.722	0.812	3.924×10^{-9}	0.752	0	
	11.0	0.04	8.2	5.981×10^9	0.26	6.558	1.239	3.17×10^{-8}	0.546	0	
	11.0	0.04	10.0	5.567×10^8	0.551	8.704	1.825	5.450×10^{-8}	0.502	0	
Calcite***	9.2	0.018	2.3	8.346×10^{10}	0.246	4.951	0.619	7.605×10^{-10}	0.822	0	
China clay****	2.9	0.125	3.3	8.318×10^{10}	0.649	2.695	0.499	2.865×10^{-8}	0.168	0	
	5.2	0.125	1.3	8.649×10^{10}	0.648	2.968	0.546	8.186×10^{-9}	0.263	0	
	5.2	0.125	3.3	4.018×10^{11}	0.458	2.521	0.446	1.288×10^{-9}	0.533	0	
	5.2	0.125	5.4	5.572×10^{11}	0.581	2.491	0.469	7.148×10^{-8}	0.116	0	
	†	5.2	0.125	floc			2.955	0.54			
	††	10.2	0.125	3.3	7.532×10^{11}	0.613	2.567	0.469	2.747×10^{-10}	0.499	0
Hydromagnesite*											
	9.9	0.07	16.4	1.044×10^{10}	0.564	12.00	2.636	4.108×10^{-7}	-0.08	1.76	

*Applied pressure range 300 to 11,000 kPa; **Applied pressure range 200 to 1000 kPa

Applied pressure range 130 to 2100 kPa; *Applied pressure range 300 to 20,000 kPa

†Suspension flocculated by Magnafloc 351 (from Allied Colloids)

††Only the voids ratio data for all pH's form a common line

Units: ⁽¹⁾ μm ; ⁽²⁾ $\text{m kg}^{-1} \text{Pa}^{-n}$; ⁽³⁾ $\text{m}^2 \text{s}^{-1} \text{kPa}^{-\gamma}$; ⁽⁴⁾ kPa

Table 1: Coefficients of the constitutive equations for the systems studied.

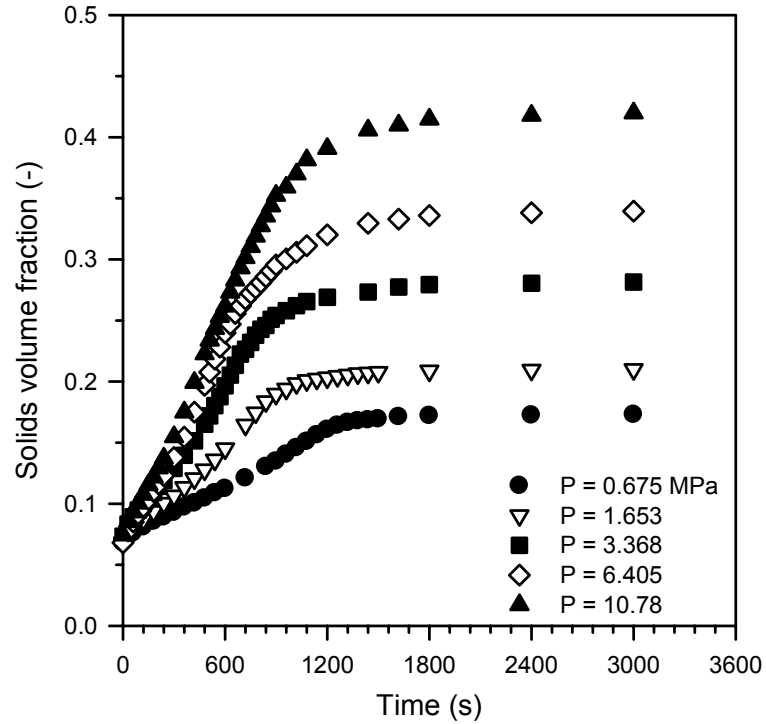


Figure 1: Effect of pressure on hydromagnesite expression.

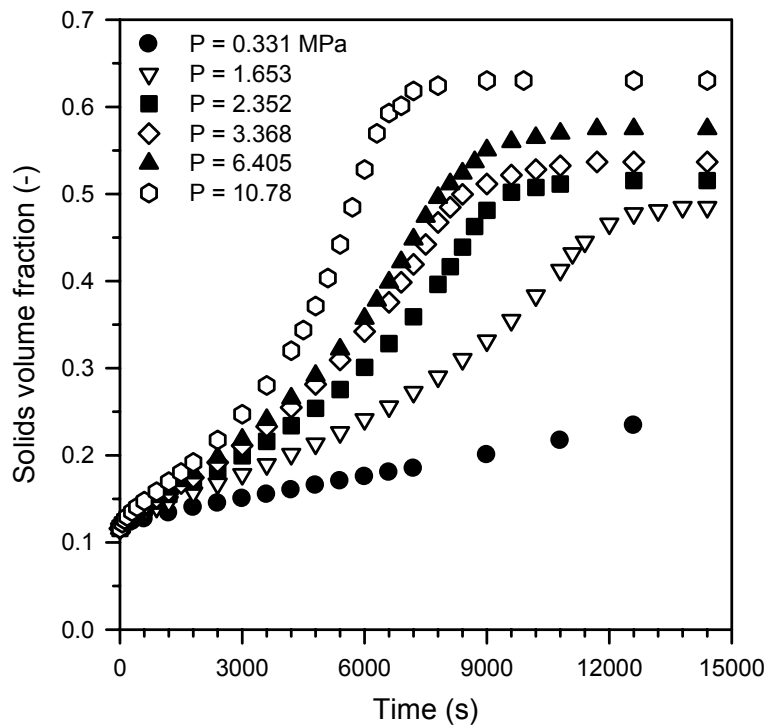


Figure 2: Effect of pressure on china clay expression.

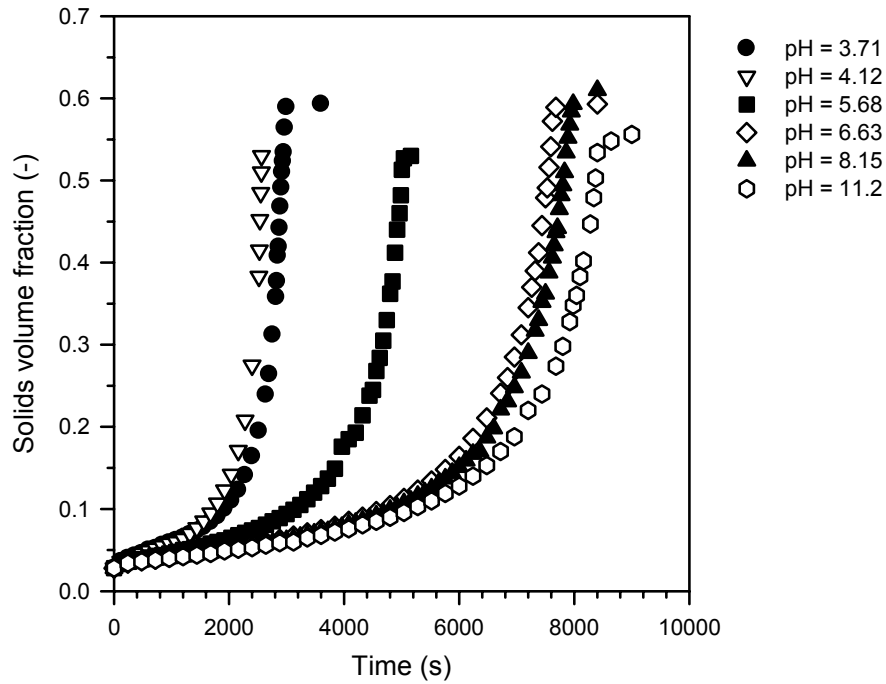


Figure 3: Effect of pH on unwashed anatase expression.

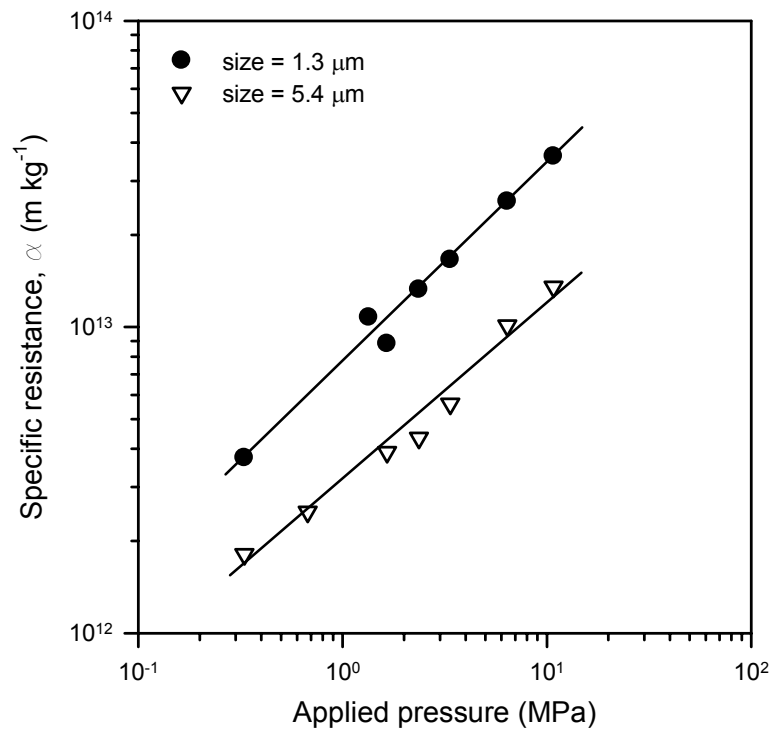


Figure 4: Dependence of α of china clay cakes on Δp and particle size.

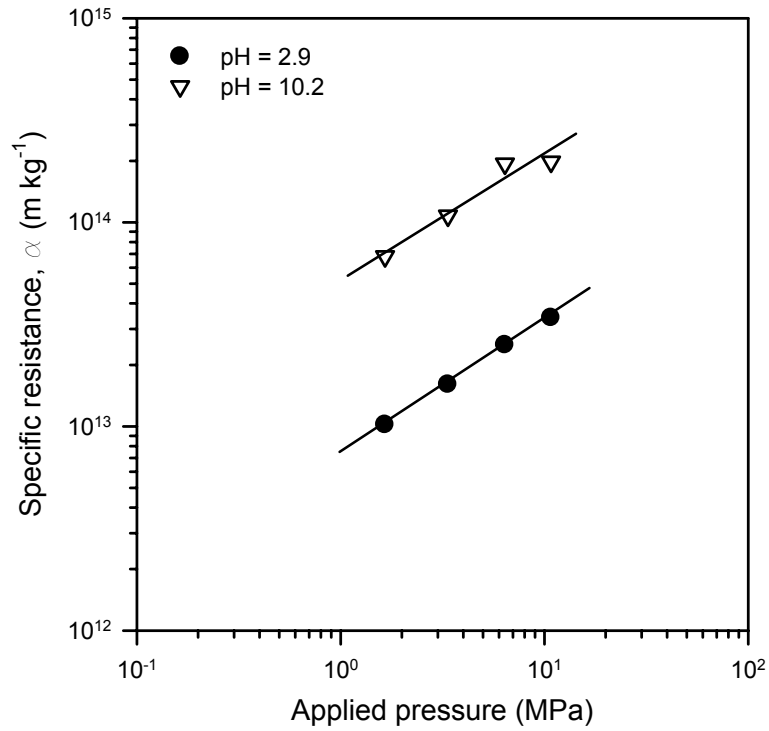


Figure 5: Dependence of α of china clay cakes on Δp and pH

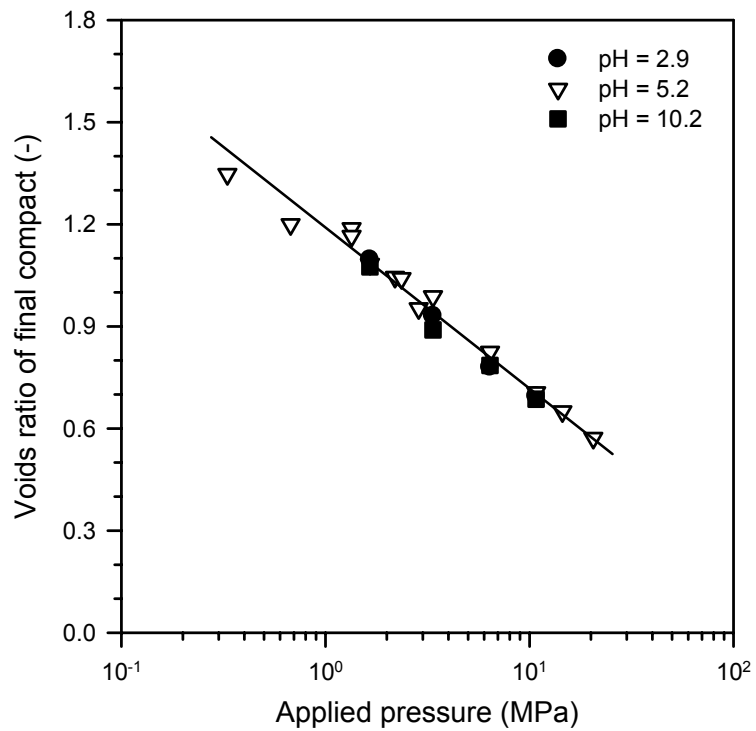


Figure 6: Dependence of ultimate voids ratio of china clay cakes on pressure and pH.

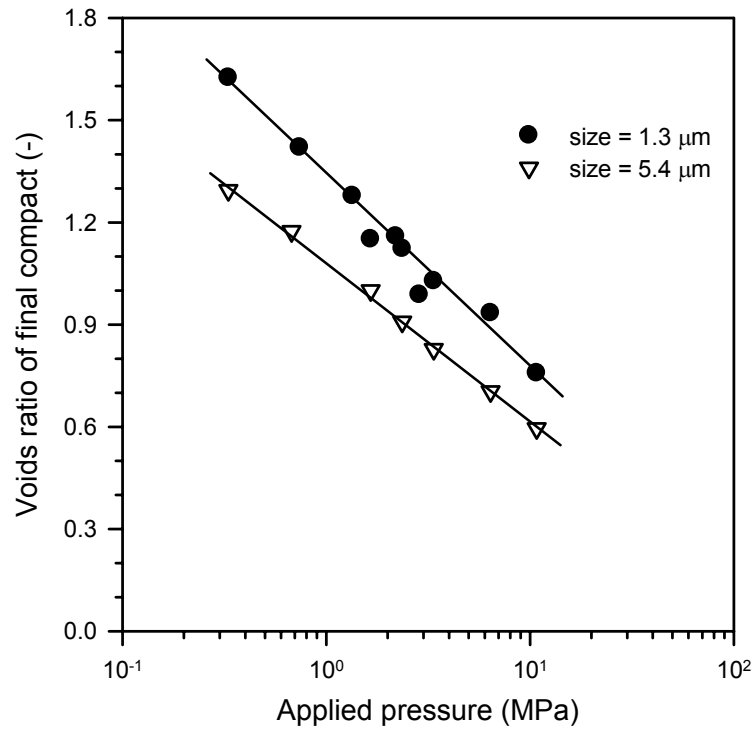


Figure 7: Dependence of ultimate voids ratio of china clay cakes on pressure and particle size.